

Magnetic interactions in the $S = 1/2$ square-lattice antiferromagnets $\text{Ba}_2\text{CuTeO}_6$ and Ba_2CuWO_6

Otto Mustonen,^{ab} Sami Vasala,^{cd} Heather Mutch,^b Chris I. Thomas,^a Gavin B. G. Stenning,^e Elisa Baggio-Saitovitch,^c Edmund J. Cussen^b and Maarit Karppinen^{*a}

Electronic Supporting Information

Density functional theory calculations

Density functional theory was used to calculate the magnetic exchange constants in $\text{Ba}_2\text{CuTeO}_6$ and Ba_2CuWO_6 . The calculations were carried out with the full potential linearized augmented plane wave code ELK.¹ We used the generalized gradient approximation functionals by Perdew, Burke and Ernzerhof.² Five different spin configurations with $2 \times 2 \times 1$ ($1 \times 1 \times 2$) supercells were needed to calculate the exchange constants (Fig. 1).^{3,4} A k point grid of $4 \times 4 \times 6$ ($8 \times 8 \times 3$) was used. A plane-wave cutoff of $|G + k|_{\text{max}} = 8/R_{\text{MT}}$ a.u.⁻¹ was used, where R_{MT} was the average muffin tin radius. Electron correlation effects of the localized Cu^{2+} $3d$ orbitals were included within the DFT+ U framework with the on-site coulombic repulsion U and Hund exchange term I as parameters.⁵ The on-site coulombic U term was varied from 7 to 9 eV, which are typical values for Cu $3d$ orbitals. The Hund term I was fixed at 0.9 eV for all calculations.

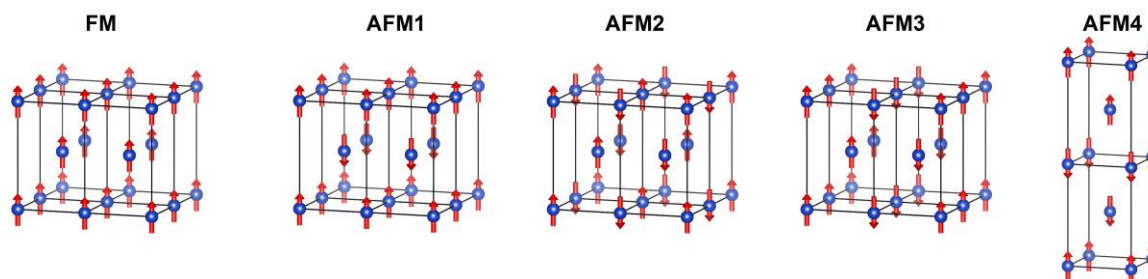


Fig. 1. The five different spin configurations used in the density functional theory calculations. Only the magnetic Cu^{2+} cations and their spins are shown. The energies are calculated in $2 \times 2 \times 1$ (and one $1 \times 1 \times 2$) supercells.

In order to obtain the exchange constants J_1 - J_4 we mapped the energies of the different spin configurations to a simple Heisenberg Hamiltonian:

$$H = - \sum_{i < j} J_{ij} S_i \cdot S_j$$

where J_{ij} is the exchange constant for the interaction between spins i and j . The spin configurations are presented in Fig. 1. Using the Hamiltonian, the energies of the spin configurations³ can be written as:

$$E_{FM} = E_0 + (-4J_1 - 4J_2 - 8J_3 - 2J_4)S^2$$

$$E_{AFM1} = E_0 + (-4J_1 - 4J_2 + 8J_3 - 2J_4)S^2$$

$$E_{AFM2} = E_0 + (4J_1 - 4J_2 - 2J_4)S^2$$

$$E_{AFM3} = E_0 + (4J_2 - 2J_4)S^2$$

$$E_{AFM4} = E_0 + (-4J_1 - 4J_2 + 2J_4)S^2$$

The exchange constants J_1 - J_4 can then be obtained from:³

$$J_3 = (E_{AFM1} - E_{FM})/16S^2$$

$$J_1 = (E_{AFM2} - E_{FM} - 8J_3S^2)/8S^2$$

$$J_2 = (E_{AFM3} - E_{FM} - 4J_1S^2 - 8J_3S^2)/8S^2$$

$$J_4 = (E_{AFM4} - E_{FM} - 8J_3S^2)/4S^2$$

The calculated energies and exchange constants for $U = 7$ - 9 eV are presented in Table 1.

Table 1. Relative total energies of the different spin configurations of $\text{Ba}_2\text{CuTeO}_6$ and Ba_2CuWO_6 calculated by density functional theory. Energy of the ferromagnetic configuration is set as zero.

	Ba₂CuTeO₆			Ba₂CuWO₆		
	$U = 7$ eV	$U = 8$ eV	$U = 9$ eV	$U = 7$ eV	$U = 8$ eV	$U = 9$ eV
E_{FM} (meV/2f.u.)	0	0	0	0	0	0
E_{AFM1} (meV/2f.u.)	5.12	3.33	2.67	0.22	-0.04	0.04
E_{AFM2} (meV/2f.u.)	-44.74	-38.78	-33.11	-2.39	-2.37	-2.51
E_{AFM3} (meV/2f.u.)	-20.82	-18.10	-15.77	-30.56	-25.08	-20.36
E_{AFM4} (meV/2f.u.)	2.26	1.67	1.39	0.14	0.35	0.04
J_1 (meV)	-23.65	-20.22	-17.22	-1.25	-1.17	-1.27
J_2 (meV)	0.13	0.23	0.06	-14.71	-11.94	-9.56
J_3 (meV)	1.28	0.83	0.67	0.05	-0.01	0.01
J_4 (meV)	-0.30	0.01	0.05	0.03	0.37	0.02
J_2/J_1	-0.01	-0.01	0.00	11.79	10.18	7.55

Structural effects on magnetic interactions

Changing strontium to barium has two effects on the structure that could explain the changes in magnetic interactions: it changes the Cu-O bond length and the Cu-O-Te/W bond angle in the ab plane, see Fig. 2 a). The equatorial Cu-O bonds in the ab plane are longer in the Ba-phases (2.01 vs 1.95 Å) but the Te/W-O bonds remain constant within experimental error. This lengthening of the Cu-O bond, on its own, would be expected to weaken the magnetic interactions in these materials. The other effect is related to the a^0a^0c octahedral tilting in these $I4/m$ double perovskites. The CuO_6 octahedrons tilt with c as the tilting axis, so that the Cu-O-Te/W angles in the ab plane are reduced from the ideal 180° (no octahedral tilting, $I4/mmm$). The larger size of the Ba^{2+} cation reduces this octahedral tilting, so that the Cu-O-Te/W angle in the ab plane is higher. This larger Cu-O-Te/W angle increases orbital overlap, and results in the observed significantly increased magnetic interactions in the Ba-phases in comparison to the Sr-phases.⁶ This effect is especially

strong in $\text{Sr}_2\text{CuTeO}_6$ and $\text{Ba}_2\text{CuTeO}_6$, where the Cu-O-Te bond angle increases from 158° to 175° when replacing strontium with barium, and as a consequence J_1 increases from -7.18 meV to -20.22 meV. The trends in bond lengths, angles and magnetic interactions are plotted in Fig. 2 panels b) and c). The trends in the Curie-Weiss constant and dominant magnetic interactions in Fig. 2 c) follow the trend in the Cu-O-Te/W angle in Fig. 2 b).

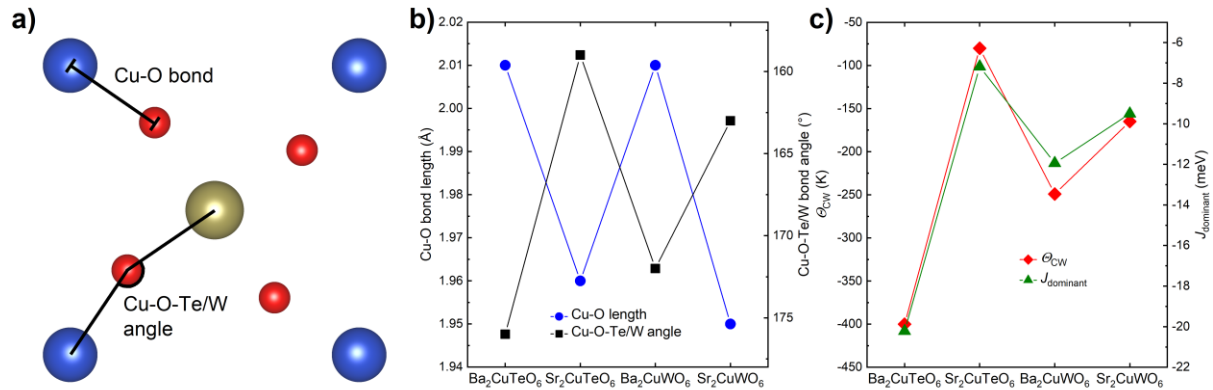


Fig. 2. a) The structure of tetragonal $\text{A}_2\text{CuB}''\text{O}_6$ double perovskites with view down the c -axis. The Cu-O bond length and the Cu-O-Te/W angle are shown. b) The Cu-O bond length and Cu-O-Te/W angle in the compounds. c) The Curie-Weiss constant and dominant magnetic interactions (J_1 for $\text{Ba}_2\text{CuTeO}_6$ and $\text{Sr}_2\text{CuTeO}_6$, J_2 for Ba_2CuWO_6 and Sr_2CuWO_6). Figure adapted from ref. 6 with data from this work and refs. 4,6–8.

Sample synthesis

Ba_2CuWO_6 and triclinic $\text{Ba}_2\text{CuTeO}_6$ were prepared using a conventional solid state reaction method from stoichiometric amounts of BaCO_3 , CuO , WO_3 and TeO_2 (Alpha Aesar ≥ 99.995). The samples were calcined at 900°C in air for 12 hours, reground, pelletized and fired twice at 1000°C in air for 24 hours. Tetragonal double perovskite $\text{Ba}_2\text{CuTeO}_6$ was prepared from triclinic $\text{Ba}_2\text{CuTeO}_6$ under high-pressure high-temperature conditions. Sample powder enclosed in a gold capsule was pressed in a cubic-anvil Riken-Seiki high-pressure apparatus at 4 GPa and 900°C for 30 min. The temperature was slowly cooled before gradually releasing the pressure. This procedure resulted in around 50 mg of sample powder.

X-ray diffraction

The phase purity of samples was investigated by x-ray diffraction. The diffraction data were collected on a Panalytical X'pert Pro MPD diffractometer using $\text{Cu } K_{\alpha 1}$ radiation. The diffraction patterns were refined with the FULLPROF⁹ software suite. Rietveld refinement was carried out for both compounds, although the data quality for $\text{Ba}_2\text{CuTeO}_6$ was not as good due to the small amount of sample powder. The crystal structures were visualized with VESTA.¹⁰

The measured x-ray diffraction patterns for $\text{Ba}_2\text{CuTeO}_6$ and Ba_2CuWO_6 are shown in Fig. 3. No impurity peaks are observed in $\text{Ba}_2\text{CuTeO}_6$ indicating that the material is phase pure. In the Ba_2CuWO_6 sample a minor ($< 1\%$) BaWO_4 impurity is observed in addition to the main phase. The lattice parameters are in good agreement with literature.⁶

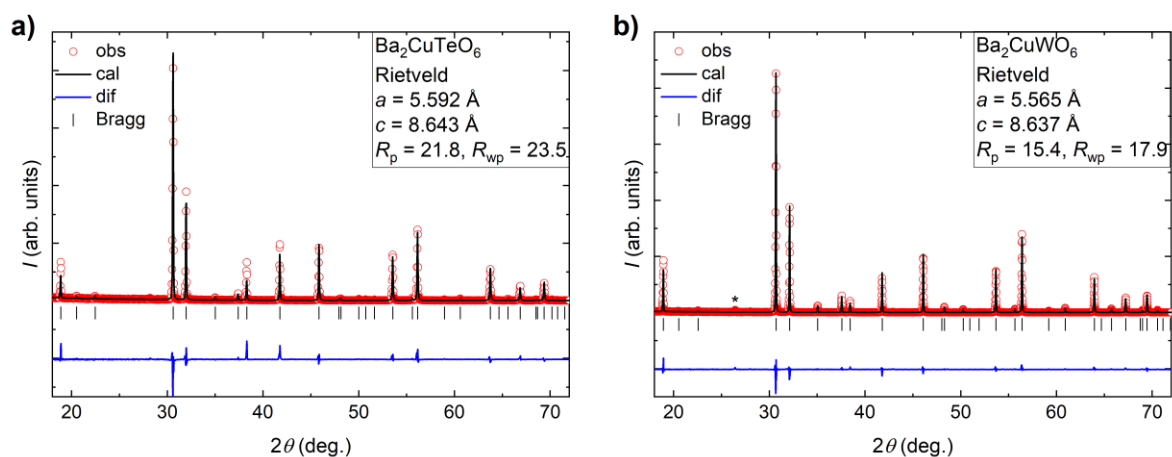


Fig. 3. X-ray diffraction patterns of (a) $\text{Ba}_2\text{CuTeO}_6$ and (b) Ba_2CuWO_6 . The minor BaWO_4 impurity in Ba_2CuWO_6 is marked with an asterisk. Bragg positions for the space group $I4/m$ are shown.

Magnetic measurements

Magnetic properties were measured with a Quantum Design MPMS3 SQUID magnetometer. 120 mg of Ba_2CuWO_6 and 25 mg of $\text{Ba}_2\text{CuTeO}_6$ were enclosed in gelatin capsules and placed in plastic straws for measurements. DC magnetic susceptibility was measured in the temperature range 2–400 K under an applied field of 1 T in zero-field cool (ZFC) and field cool (FC) modes.

References

- 1 <http://elk.sourceforge.net>.
- 2 J. P. Perdew, K. Burke and M. Ernzerhof, *Phys. Rev. Lett.*, 1996, **77**, 3865–3868.
- 3 S. Vasala, H. Saadaoui, E. Morenzoni, O. Chmaissem, T. Chan, J. Chen, Y. Hsu, H. Yamauchi and M. Karppinen, *Phys. Rev. B*, 2014, **89**, 134419.
- 4 H. C. Walker, O. Mustonen, S. Vasala, D. J. Voneshen, M. D. Le, D. T. Adroja and M. Karppinen, *Phys. Rev. B*, 2016, **94**, 064411.
- 5 A. I. Liechtenstein, V. I. Anisimov and J. Zaanen, *Phys. Rev. B*, 1995, **52**, R5467–R5470.
- 6 D. Iwanaga, Y. Inaguma and M. Itoh, *J. Solid State Chem.*, 1999, **147**, 291–295.
- 7 P. Babkevich, V. M. Katukuri, B. Fåk, S. Rols, T. Fennell, D. Pajić, H. Tanaka, T. Pardini, R. R. P. Singh, A. Mitrushchenkov, O. V. Yazyev and H. M. Rønnow, *Phys. Rev. Lett.*, 2016, **117**, 237203.
- 8 O. Mustonen, S. Vasala, E. Sadrollahi, K. P. Schmidt, C. Baines, H. C. Walker, I. Terasaki, F. J. Litterst, E. Baggio-Saitovitch and M. Karppinen, *Nat. Commun.*, 2018, **9**, 1085.
- 9 J. Rodríguez-Carvajal, *Phys. B*, 1993, **192**, 55–69.
- 10 K. Momma and F. Izumi, *J. Appl. Crystallogr.*, 2011, **44**, 1272–1276.